

---

01 Jun 2022

## Application of Leeb Hardness Test in Prediction of Dynamic Elastic Constants of Sedimentary and Igneous Rocks

Sasan Ghorbani

Seyed Hadi Hoseinie

Ebrahim Ghasemi

Taghi Sherizadeh

Missouri University of Science and Technology, sherizadeh@mst.edu

Follow this and additional works at: [https://scholarsmine.mst.edu/min\\_nuceng\\_facwork](https://scholarsmine.mst.edu/min_nuceng_facwork)



Part of the [Mining Engineering Commons](#)

---

### Recommended Citation

S. Ghorbani et al., "Application of Leeb Hardness Test in Prediction of Dynamic Elastic Constants of Sedimentary and Igneous Rocks," *Geotechnical and Geological Engineering*, vol. 40, no. 6, pp. 3125 - 3145, Springer, Jun 2022.

The definitive version is available at <https://doi.org/10.1007/s10706-022-02083-z>

This Article - Journal is brought to you for free and open access by Scholars' Mine. It has been accepted for inclusion in Mining Engineering Faculty Research & Creative Works by an authorized administrator of Scholars' Mine. This work is protected by U. S. Copyright Law. Unauthorized use including reproduction for redistribution requires the permission of the copyright holder. For more information, please contact [scholarsmine@mst.edu](mailto:scholarsmine@mst.edu).



# Application of Leeb Hardness Test in Prediction of Dynamic Elastic Constants of Sedimentary and Igneous Rocks

Sasan Ghorbani · Seyed Hadi Hoseinie ·  
Ebrahim Ghasemi · Taghi Sherizadeh

Received: 29 December 2021 / Accepted: 7 February 2022 / Published online: 2 March 2022  
© The Author(s), under exclusive licence to Springer Nature Switzerland AG 2022

**Abstract** The Leeb hardness test is a non-destructive and portable technique that can be used both in the laboratory and in-field applications. The main purpose of this study is to predict the dynamic elastic constants of the igneous and sedimentary rocks using Leeb dynamic hardness testing. For this purpose, three vital topics have been investigated and analyzed. First, the relationships between ultrasonic wave velocities and dynamic elastic constants with the Leeb hardness were investigated. Thereafter, by determining the rock quality index (IQ) using microscopic studies and by analyzing the quality index-porosity plot, the variation of the Leeb hardness values was studied. Eventually, the longitudinal waveform in rock samples with different quality indexes and Leeb hardness were analyzed. To achieve these outputs, 33 samples of igneous and sedimentary rocks with a wide range of physical, mechanical, and textural features were collected and tested. The results of the analyses show that in both igneous and sedimentary rocks, the dynamic modulus of elasticity ( $E_d$ ) has a significant correlation with the Leeb hardness. Generally, based on the microscopic studies, it was

observed that the existence of the porosity in sedimentary rocks and intercrystalline and intracrystalline fissures in igneous rocks sharply reduce the Leeb hardness and thus lead to changes in the form of the longitudinal waves.

**Keywords** Leeb hardness · Dynamic elastic constants · Non-destructive technique · Quality index · Longitudinal waveform

## 1 Introduction

An accurate estimation of dynamic elastic constants is vital for almost any form of design and analysis in rock, civil, and geological engineering projects (Diamantis et al. 2009; Azimian 2017; Jamshidi and Torabi-Kaveh 2021). Among dynamic elastic constants, modulus of elasticity, modulus of rigidity, and bulk modulus are the fundamental ones (Davaranah et al. 2020). The empirical equations can be implemented to get the quick and almost accurate estimation of dynamic elastic constants, especially at the field applications. Non-destructive hardness tests are such useful indirect methods that could be applied for the assessment of dynamic elastic constants.

All rock hardness tests are classified based on their testing mechanisms in four categories: rebound, indentation, scratch, and grinding. The methods which apply rebound mechanisms are called “dynamic” and are more applicable and

---

S. Ghorbani · S. H. Hoseinie (✉) · E. Ghasemi  
Department of Mining Engineering, Isfahan University  
of Technology, Isfahan 84156-83111, Iran  
e-mail: hadi.hoseinie@iut.ac.ir

T. Sherizadeh  
Department of Mining and Nuclear Engineering, Missouri  
University of Science and Technology, Rolla, USA

less restrictive than other mechanisms. In general, Schmidt hammer, Shore scleroscope, and Leeb hardness which are classified in rebound-based methods are widely used in rock mechanics and civil engineering due to the economical and practical compared to the indentation-based hardness test methods such as Brinell, Vickers, Rockwell, Knoop, etc. (Çelik and Çobanoğlu 2019).

Leeb (or Equotip) hardness test has been introduced by Leeb (1978) and was originally developed for measuring the hardness of metallic materials. This test is portable, precise, and non-destructive (based on the low impact force) (Aoki and Matsukura 2007; Desarnaud et al. 2019; Gomez-Heras et al. 2020). Generally, due to the dynamic nature of rebound-based hardness tests, they could be significantly applied for the estimation of dynamical characteristics of rocks (Gupta 2009; Yagiz 2009; Sharma et al. 2011; Khandelwal 2013; Sousa 2014; Karaman and Kesimal 2015). The Leeb hardness test can be carried out rapidly, conveniently, and non-destructively on core and block samples or rock outcrops. This makes the Leeb hardness device convenient for field tests (Hack et al. 1993; Viles et al. 2011; Yilmaz 2013; Garrido et al. 2021; İnce and Bozdağ 2021).

The estimation of rock physical and mechanical properties using Leeb hardness is widely used in rock mechanics. Numerous authors have presented correlations between UCS, Young's modulus, density, porosity, and  $V_p$  with Leeb hardness (Meulenkamp and Grima 1999; Aoki and Matsukura 2008; Yilmaz and Goktan 2018; Corkum et al. 2018; Yüksek 2019; Çelik and Çobanoğlu 2019; Aldeeky et al. 2020; Çelik et al. 2020; Gomez-Heras et al. 2020; Benavente et al. 2021; Garrido et al. 2021; İnce and Bozdağ 2021). But no research is available on dynamic elastic constants prediction for rocks using Leeb hardness. Meulenkamp and Grima (1999) performed a study on 194 different rock samples to estimate the UCS value using Leeb hardness, porosity, density, grain size, and lithology of rocks with the neural network method. Aoki and Matsukura (2008) estimated UCS using Leeb hardness with a good correlation coefficient. However, they concluded that the estimation of UCS is more meaningful when Leeb hardness and porosity values were used together. Corkum et al. (2018) investigated the relationships between  $\sigma_c$  of igneous, sedimentary, and metamorphic rock types using the Leeb hardness test. They

found reasonable power correlations. Additionally, their results showed that the Leeb hardness test can be useful for field estimation of  $\sigma_c$ . Yilmaz and Goktan (2018) investigated the relationship between UCS, open porosity, and apparent density with Leeb hardness by employing an 'Arch-shaped' and a 'V-shaped' core holders. Their statistical analyses show that the UCS could reliably be estimated by employing any of the holders. In contrast, the porosity and density of the tested rock samples were not significantly correlated to the Leeb hardness obtained in the two holders. Çelik and Çobanoğlu (2019) also examined the correlations between dry unit weight, open porosity, water absorption, wide wheel abrasion, and UCS with Leeb, Shore, and Schmidt hardness tests. They concluded that the Leeb hardness test in rock material characterization is more useful than the Schmidt and Shore hardness tests. Yüksek (2019) found reasonable correlations between UCS, dry unit weight, porosity, and water absorption with Leeb hardness of six volcanic building stones. Çelik et al. (2020) investigated the relationships between the dry and saturated unit volume weights, apparent porosity, water absorption  $V_p$ , and UCS with Leeb hardness. They proposed the regression equations with high correlation coefficients. Gomez-Heras et al. (2020) provided a way to estimate the UCS by combining the Leeb hardness test and ultrasonic pulse velocity. They concluded that combining ultrasonic pulse velocity and Leeb hardness is an effective way to improve UCS estimations. Aldeeky et al. (2020) provided the relationships between UCS and Young's modulus of basalt rock with the Leeb hardness. They found a strong power correlation ( $R^2=0.88$ ) between Leeb hardness and UCS and a good linear correlation ( $R^2=0.79$ ) between Young's modulus and Leeb hardness. Garrido et al. (2021) predicted the UCS of limestone samples using Leeb hardness. They first heated the samples at different temperatures, including 105, 200, 300, 400, 500, 600, 700, 800, and 900 °C, and then cooled them in two modes, slow and quick. They provided relationships for predicting UCS in both modes with significant regression coefficients. İnce and Bozdağ (2021) analyzed the correlation between  $V_p$ , dry density, porosity, and UCS with dry and saturated Leeb hardness. They used 76 various types of magmatic rock samples. Their statistical analyses showed that the highest correlation coefficients between the dry and saturated Leeb hardness are with

the porosity and UCS, respectively. Benavente et al. (2021) conducted a study on carbonate sedimentary rocks to estimate the UCS by combining open porosity,  $V_p$ , Leeb hardness, and micro-drilling resistance force with multiple regression expressions.

This paper, it is tried to predict the dynamic elastic constants of the sedimentary and igneous rocks using the Leeb hardness test as the fastest and most portable dynamic rock hardness testing technique. In the next step, the interaction between the quality index (IQ) of rocks and their Leeb hardness values is studied and investigated as well. Finally, the longitudinal wave-form in different classes of the Leeb hardness and IQ is also measured and evaluated.

## 2 Theoretical Background and Measuring Techniques

### 2.1 Leeb Dynamic Hardness

The Leeb device is provided digitally and with very small instruments for measuring the dynamic hardness of steel products (ASTM A956-06 2006). This method is considered a highly portable, fast, cost-effective, and convenient method for field applications (Corkum et al. 2018).

In general, the D-type impact body of the Leeb hardness instrument is commonly used in rock engineering applications (Çelik and Çobanoğlu 2019).

To perform the Leeb hardness tests in the current research, the ITI-130 Leeb instrument (D1+type) was used (see Fig. 1a). Additionally, the circular measuring pattern on the core samples' surfaces was applied for hardness measurements as shown in Fig. 1(b). The Leeb hardness value (L.H) is calculated by dividing the rebound velocity by the impact velocity as shown in Fig. 1(c).

### 2.2 Dynamic Elastic Constants

As a non-destructive test method, longitudinal and shear wave velocities ( $V_p$  and  $V_s$ ) values of rocks are widely used in the calculating of dynamic elastic characterizations of rocks viewpoint of economic and practical advantages (Jamshidi and Yazarloo 2021).

$V_p$  and  $V_s$  in the current research were determined by the ultrasonic pulse transmission technique. In upgrade suggested method covers the two approaches, the so-called high (100 kHz-2 MHz) and low (2–30 kHz) frequency ultrasonic pulse techniques. In the pulse method of ultrasonic testing, generating sound wave trains and detecting their propagation through solids can be achieved by a single transducer (pulse-echo technique) or by a pair of transducers (pitch-catch technique). The basic configurations of transducer pairs (transmitter–receiver) used in the pitch-catch technique include direct (through) transmission, indirect (surface) transmission, and semi-direct (edge) transmission (ISRM 2015).

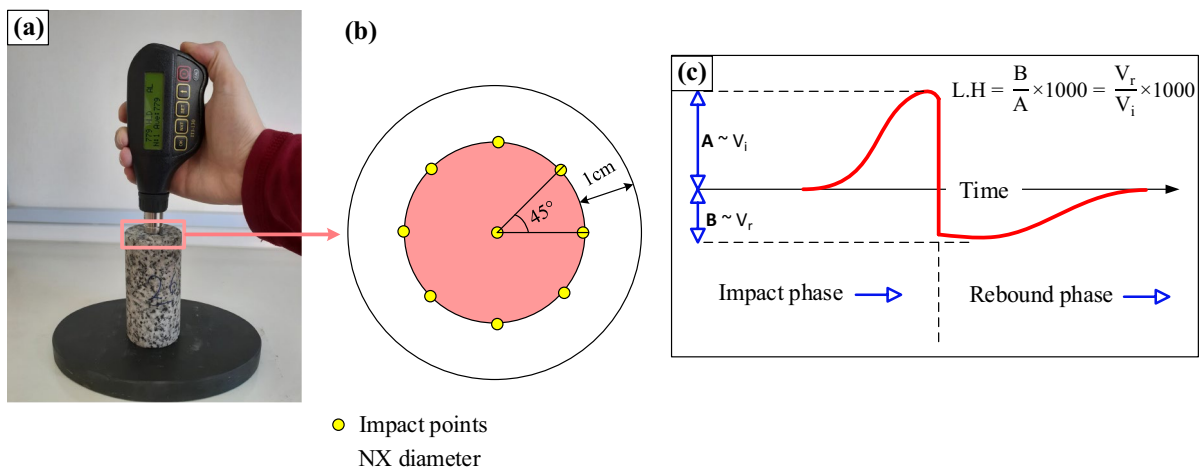


**Fig. 1** Leeb hardness testing equipment (a) ITI 130 Leeb hardness tester (b) circular testing pattern (c) typical generated voltage curve (Frank et al. 2019)

In order to determine the  $V_p$  and  $V_s$ , in this study, a Portable Ultrasonic Non-destructive Digital Indicating Tester (PUNDIT Lab+) instrument and two transducers (a transmitter and a receiver) having a frequency of 500 kHz (high-frequency method) and direct transmission configuration were used. In this approach, after calibrating the instrument with the calibration bar, the transmitter excitation signal travels through the length of the sample, and the oscilloscope records wave traveling time. The time that is detected by oscilloscope for the first time at the beginning of the  $V_p$  form is taken into account as  $t_p$  (Dehghani et al. 2020). Three tests were performed for each type of rock and the mean value of the  $V_p$  and  $V_s$  of each sample were considered.

After the measurement of  $V_p$  and  $V_s$  of rock samples, the dynamic elastic constants including modulus of elasticity, modulus of rigidity, and bulk modulus have been calculated using Eqs. (1–4) (Martínez-Martínez et al. 2012; Ajalloeian et al. 2020).

$$E_{\text{dyn}} = \frac{\rho V_s^2 (3V_p^2 - 4V_s^2)}{V_p^2 - V_s^2} \quad (1)$$

$$\vartheta_{\text{dyn}} = \frac{V_p^2 - 2V_s^2}{2(V_p^2 - V_s^2)} \quad (2)$$

$$G_{\text{dyn}} = \frac{E_{\text{dyn}}}{2(1 + \vartheta_{\text{dyn}})} \quad (3)$$

$$K_{\text{dyn}} = \frac{E_{\text{dyn}}}{3(1 - 2\vartheta_{\text{dyn}})} \quad (4)$$

where  $E_{\text{dyn}}$ , is the dynamic modulus of elasticity (GPa),  $G_{\text{dyn}}$ , is the dynamic modulus of rigidity (GPa),  $K_{\text{dyn}}$ , is dynamic bulk modulus (GPa),  $\vartheta_{\text{dyn}}$ , is dynamic Poisson's ratio,  $\rho$ , is density ( $\text{g/cm}^3$ ) and  $V_p$  and  $V_s$  are in Km/s.

### 2.3 Quality Index (IQ)

Fissures and micro-fractures in intact rocks are the most important parameters affecting ultrasonic wave velocity. The presence of fissures increases the rock porosity and decreases the ultrasonic wave velocity. Thus, the wave velocity could be applied to analyze

the degree of fissuring within rock specimens indirectly (Goodman 1989; Fereidooni 2018). In practice, a network of fissures in the sample imposes a fundamental effect on the mechanical properties of the rock such as dynamic constants and hardness.

In this paper, the IQ values are analyzed according to the model proposed by Fourmaintraux (1976). In this procedure, the  $V_p$  of the sample ( $V_1^*$ , without considering the pores or fissures in the rock) is calculated according to Eq. (5). Finally, the ratio of  $V_1/V_1^*$  is calculated and reported as the quality index (Eq. 6).

$$\frac{1}{V_1^*} = \sum_i \frac{C_i}{V_{1,i}} \quad (5)$$

$$\text{IQ} (\%) = \frac{V_1}{V_1^*} \quad (6)$$

where  $V_{1,i}$  is the  $V_p$  in mineral constituent  $i$ ,  $C_i$  is the percent of rock's minerals, and  $V_1$  is the measured  $V_p$ .

Because of the extreme sensitivity of IQ to fissuring, Fourmaintraux proposed plotting IQ versus porosity as a basis for describing the degree of fissuring of a rock sample. Based on the porosity value and calculated IQ, a data point is classified into one of the five following categories (Goodman 1989):

- (1) Non-fissured to slightly fissured
- (2) Slightly to moderately fissured
- (3) Moderately to strongly fissured
- (4) Strongly to very strongly fissured
- (5) Extremely fissured

## 3 Laboratorial Analysis

### 3.1 Samples Preparation

During this study, a set of 33 various rock types with fundamentally different physical, mechanical, textural, and geological origins were analyzed and studied. These samples were carefully selected to avoid any signs of weathering. The required samples for  $V_p$  and  $V_s$  tests were prepared according to the ISRM suggested methods (ISRM 2015) with 54 mm core diameter (length to diameter ratio of 2). Also, to calculate the IQ of the studied rocks, thin sections were

prepared and analyzed. It should be noted that the ends of the core specimens were flattened completely.

### 3.2 Measurement of the Leeb Hardness

To determine the Leeb hardness values in each sample, a single impact method (SIM) using a circular testing pattern was implemented on the core samples with a length to diameter ratio of 2. Eighteen single impacts were performed on each sample, and the average of these impact numbers was assigned as the Leeb hardness number (see Fig. 1) for each rock type. All samples are placed on the holder and Leeb tests were performed in the vertical position on the core surfaces. The results of the Leeb hardness tests are presented in Table 1.

### 3.3 Determining the Dynamic Elastic Constants

The values of dynamic elastic constants of the studied rocks were calculated based on the values of  $V_p$ ,  $V_s$ , and density and using Eqs. (1–4). The name of the studied rocks, sample number, and the values of the porosity, density, and calculated dynamic elastic constants are presented in Table 1. It should be mentioned that the physical tests including porosity and density were determined using the ISRM standard methods (ISRM 1981).

### 3.4 Mineralogical Studies

The engineering behavior of rocks is closely related to their mineralogical content and internal composition (Fereidooni 2018). Additionally, the rock texture influences its engineering properties (Bandini and Berry 2013). Therefore, in this paper, mineralogical studies have been performed to calculate the quality index of the rocks.

In this study, 33 thin sections in total from the studied sedimentary and igneous samples were examined under a polarization microscope (BH2 series) with crossed polarized light (XPL) to determine the petrographic characteristics. Microphotographs of thin sections were taken using a digital camera mounted on a petrographic microscope. The microscope is equipped with an analyzer and polarizer that might be rotated independently. After taking microphotographs of each thin section, the percentage of minerals is obtained from segmented photomicrographs.

In other words, the desired photomicrographs were analyzed and grain boundaries were identified and separated from the matrix. Thereafter, by coding every grain at each thin section and aggregating the mineral's results each mineral's exact contribution to the rock formation and the mineralogical composition of each rock type was determined and recorded correctly. Table 2 presents the mineralogical composition and percentages of each mineral of studied rock types. The results of petrographic analyses show that the igneous samples' dominant minerals are quartz, plagioclase, K-feldspar, amphibole, and biotite. In the sedimentary samples, there are mostly three minerals, sparite and micrite calcite, and hematite.





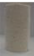


















## 4 Statistical and Regression Analysis

After performing the Leeb hardness and  $V_p$  and  $V_s$  tests, the relationships between the dynamic elastic constants and the Leeb method have been investigated to identify any possible strong interactions and correlations among them. Since the Leeb hardness is the fast and portable method, the regression analyses focused on predicting the dynamic elastic constants using the Leeb number. In the first stage, a statistical analysis was performed on calculated dynamic elastic constants to clarify the available data and probability density of them. The histograms of the  $V_p$ ,  $V_s$ , dynamic elastic constants, and Leeb dynamic hardness values are shown in Fig. 2. Some statistical information about the probability distribution of these parameters is also provided. The analyses show that these parameters all obey the approximately normal distribution and the values are in a wide range and potentially provide significant scientific background for further analysis.











### 4.1 $V_p$ and $V_s$ vs Leeb Hardness

In rock engineering and engineering geology, regression analysis is applied to develop predictive models among the relevant rock properties (Gokceoglu and Zorlu 2004; İnce and Bozdağ 2021). In this section, regression analyses were carried out to establish predictive models to assess the  $V_p$  and  $V_s$  from Leeb dynamic hardness test. Framing a correlation between a rock property and Leeb dynamic hardness test, data obtained from different rock types with different

**Table 1** Results of laboratory tests

Sample No.	Rock name	View of specimen	Leeb hardness	V <sub>p</sub> (m/s)	V <sub>s</sub> (m/s)	Density (g/cm <sup>3</sup> )	Porosity (%)	E <sub>dyn</sub> (GPa)	G <sub>dyn</sub> (GPa)	K <sub>dyn</sub> (GPa)
1	Limestone		496	5621	2819	2.46	2.21	51.9	19.6	50.4
2	Fossiliferous limestone		696	6187	2783	2.59	0.79	55	20	72.4
3	Fossiliferous limestone		657	6054	2764	2.64	1.16	55.2	20.2	69.9
4	Limestone		539	5575	3079	2.46	1.84	59.7	23.3	45.4
5	Limestone		551	5419	2687	2.54	6.31	49	18.4	50.1
6	Limestone		574	5714	2775	2.54	2.52	52.6	19.6	56.9
7	Fossiliferous limestone		508	4812	2601	2.4	6	42	16.3	33.9
8	Limestone		691	6308	3041	2.63	0.9	65.6	25.2	55.4
9	Travertine		501	5393	2616	2.52	6.39	46.4	17.2	50.3
10	Limestone		769	5915	3415	2.64	0.19	77	30.8	51.3
11	Marble		634	6234	2800	2.59	4.43	55.8	20.3	73.6
12	Dolomitic limestone		526	5132	2896	2.57	7.04	54.6	21.5	38.9
13	Salt		261	3924	1789	2.02	12	17.7	6.5	22.5
14	Cavernous limestone		563	5854	2874	2.58	2.68	57.2	21.3	60
15	Limestone		627	6164	2934	2.52	1.93	58.7	21.7	66.8
16	Limestone		589	5427	2487	2.59	7.25	43.8	16	54.9
17	Cavernous limestone		461	5330	2456	2.5	3.51	41.2	15	50.9
18	Limestone		682	6403	2714	2.63	0.43	53.9	19.4	82
19	Cavernous limestone		465	4532	2075	2.46	6.06	29	10.6	36.4
20	Travertine		391	3915	2185	2.37	3.90	28.8	11.8	17.4
21	Cavernous limestone		547	5665	2715	2.5	3.68	49.8	18.4	55.7
22	Limestone		465	4278	2421	2.32	8.61	34.4	13.6	24.3
23	Limestone		559	6033	2746	2.59	1.41	53.5	20.2	51.4

**Table 1** (continued)

Sample No.	Rock name	View of core specimen	Leeb hardness	$V_p$ (m/s)	$V_s$ (m/s)	Density (g/cm <sup>3</sup> )	Porosity (%)	$E_{dyn}$ (GPa)	$G_{dyn}$ (GPa)	$K_{dyn}$ (GPa)
24	Granodiorite		766	4475	2738	2.72	0.56	49	20.4	27.3
25	Quartz monzonite		827	5952	2885	2.77	1.13	62.1	23.9	51.8
26	Tuff		686	3750	2186	2.59	3.46	30.8	12.4	19.9
27	Rhyolite		784	4874	2622	2.53	2.39	45.1	17.4	36.9
28	Tuff		602	3265	1971	2.39	5.48	22.5	9.3	13
29	Muscovite granite		775	4435	2567	2.58	1.31	42.4	17	28
30	Granite		802	4760	2676	2.73	1.26	49.8	19.5	35.8
31	Mylonite granite		875	5241	2899	2.82	0.87	60.7	24.7	37.3
32	Sino-granite		817	5073	2467	2.6	1.33	42.6	16.4	35.3
33	Tuff		752	5025	2742	2.54	2.29	49.2	19	38.7

geology origins should not be clubbed together for any statistical correlation as mechanical responses of different rocks to the same kind of applied stress are likely to differ depending on the rock microstructures. So, regression analyses have been performed on 23 sedimentary and 10 igneous rock samples, separately.

As can be seen in Figs. 3 and 4, the relationship between  $V_p$  and  $V_s$  with Leeb's dynamic hardness in igneous rocks is more significant than sedimentary rocks. These relationships in both the sedimentary and igneous rock samples follow power functions. The denser structure and less porosity in igneous rocks are the main reasons for having a significant relationship between  $V_p$  and  $V_s$  with Leeb hardness in studied rocks.

With a closer look, as porosity increases, ultrasonic pulse velocity decreases, as it is much slower through the pore spaces than through the rock matrix. However, rocks with the same porosity may not have the same  $V_p$ ; where an extended network of micropores is present, a lower propagation velocity is recorded than in rocks with a greater prevalence of macropore spaces (Kelsall et al. 1986). Therefore, it can be concluded that the higher the porosity, the lower the  $V_p$ ,

and the lower the Leeb hardness. When the rock has more pores and cracks, this causes more complexity in the passage of sonic waves and reduces its continuity, thereby decreasing the  $V_p$  and then Leeb dynamic hardness values. The decreasing trend of the  $V_p$  of the studied igneous and sedimentary rocks based on the porosity values is shown in Fig. 5. According to this Figure, with increasing porosity in igneous and sedimentary samples, a decreasing trend of  $V_p$  is observed.

#### 4.2 Dynamic Elastic Constants Versus Leeb Hardness

In addition to the longitudinal and shear velocities, the regression analysis between dynamic elastic constants and Leeb hardness has also been performed. For this purpose, linear, logarithmic, exponential, and power curve fitting were tried and the best approximation with the highest coefficient of correlation and lowest standard error of estimate (SEE) was selected Figs. 6, 7 and 8. As can be seen in these Figures, the obtained data are divided into two clusters, sedimentary and igneous. Therefore, it is clear that the



**Table 2** Results from mineralogical and petrographic analysis of thin sections of studied rock samples

Sample No	Rock name	Sample origin	Percentage of mineral (%)																
			Sparite calcite	Micrite calcite	Hematite/Magnetite	Coral parts	Quartz/Clay	Plagioclase	K-feldspar	Amphibole	Biotite	Pyroxene	Muscovite	Opaque minerals	Halite	Other			
1	Limestone	Sedimentary	100	–	–	–	–	–	–	–	–	–	–	–	–	–	–	–	
2	Fossiliferous limestone		22	52	6	20	–	–	–	–	–	–	–	–	–	–	–	–	
3	Fossiliferous limestone		25	50	5	20	–	–	–	–	–	–	–	–	–	–	–	–	
4	Limestone		28	72	–	–	–	–	–	–	–	–	–	–	–	–	–	–	
5	Limestone		15	75	–	10	–	–	–	–	–	–	–	–	–	–	–	–	
6	Limestone		45	40	5	7	3	–	–	–	–	–	–	–	–	–	–	–	
7	Fossiliferous limestone		40	20	40	–	–	–	–	–	–	–	–	–	–	–	–	–	
8	Limestone		48	45	7	–	–	–	–	–	–	–	–	–	–	–	–	–	
9	Travertine		65	5	30	–	–	–	–	–	–	–	–	–	–	–	–	–	
10	Limestone		90	4	–	–	Q:3 C:3	–	–	–	–	–	–	–	–	–	–	–	
11	Marble		100	–	–	–	–	–	–	–	–	–	–	–	–	–	–	–	
12	Dolomitic limestone		52	38	10	–	–	–	–	–	–	–	–	–	–	–	–	–	
13	Salt		–	–	–	–	–	–	–	–	–	–	–	–	–	–	–	100	–

**Table 2** (continued)

Sample No	Rock name	Sample origin	Percentage of mineral (%)														
			Sparite calcite	Micrite calcite	Hematite/Magnetite	Coral parts	Quartz/Clay	Plagioclase	K-feldspar	Amphibole	Biotite	Pyroxene	Muscovite	Opaque minerals	Halite	Other	
14	Cavernous limestone		45	50	M=5	-	-	-	-	-	-	-	-	-	-	-	-
15	Limestone		55	30	-	15	-	-	-	-	-	-	-	-	-	-	-
16	Limestone		20	75	-	5	-	-	-	-	-	-	-	-	-	-	-
17	Cavernous limestone		48	46	4	-	2	-	-	-	-	-	-	-	-	-	-
18	Limestone		45	40	2	5	8	-	-	-	-	-	-	-	-	-	-
19	Cavernous limestone		37	57	6	-	-	-	-	-	-	-	-	-	-	-	-
20	Travertine		38	49	13	-	-	-	-	-	-	-	-	-	-	-	-
21	Cavernous limestone		66	29	3	-	2	-	-	-	-	-	-	-	-	-	-
22	Limestone		47	48	5	-	-	-	-	-	-	-	-	-	-	-	-
23	Limestone		48	47	3	-	2	-	-	-	-	-	-	-	-	-	-
24	Granodiorite	Igneous	-	-	-	-	6	55	20	12	5	-	-	2	-	-	-
25	Quartz monzonite		-	-	-	-	11	33	5	8	-	-	2	-	-	-	-

Table 2 (continued)

Sample No	Rock name	Sample origin	Percentage of mineral (%)													
			Sparite calcite	Micrite calcite	Hematite/Magnetite	Coral parts	Quartz/Clay	Plagioclase	K-feldspar	Amphibole	Biotite	Pyroxene	Muscovite	Opaque minerals	Halite	Other
26	Tuff		20	-	-	-	5	30	-	-	-	-	-	-	-	45*
27	Rhyolite		-	-	-	47	34	5	-	12	-	-	2	-	-	-
28	Tuff		10	-	-	-	Q:5 C:25	10	-	-	-	15	-	5	-	30**
29	Muscovite granite		-	-	-	-	30	15	40	-	3	-	11	1	-	-
30	Granite		-	-	-	-	21	25	30	8	15	-	-	1	-	-
31	Mylonite granite		-	-	-	-	25	15	48	-	10	-	-	2	-	-
32	Sino-granite		-	-	-	-	12	28	44	-	12	-	-	-	4**	-
33	Tuff		10	-	-	-	20	15	5	2	3	-	-	-	45**	-

\*Chlorite and clay minerals

\*\*Iron oxide, and fine-grained minerals

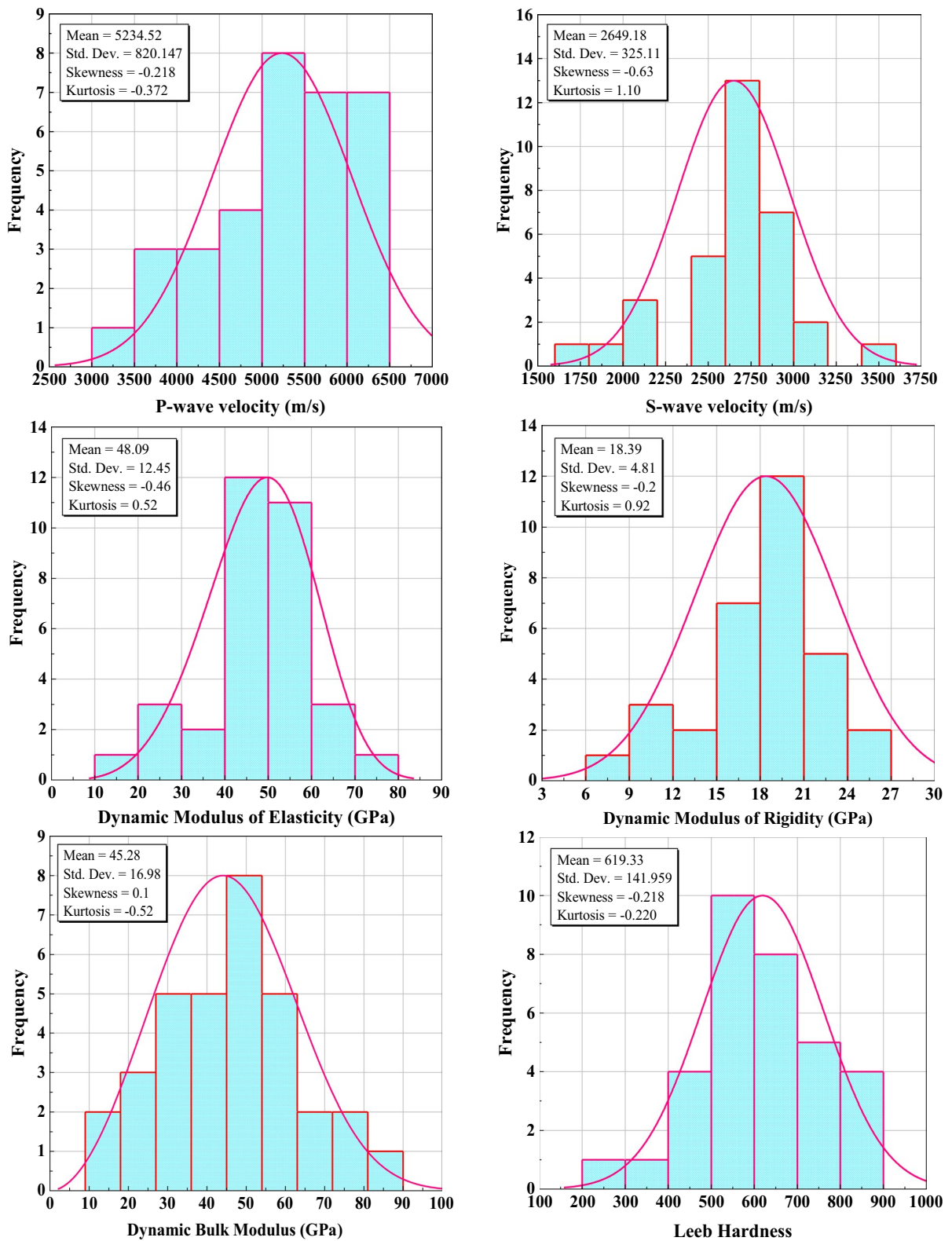
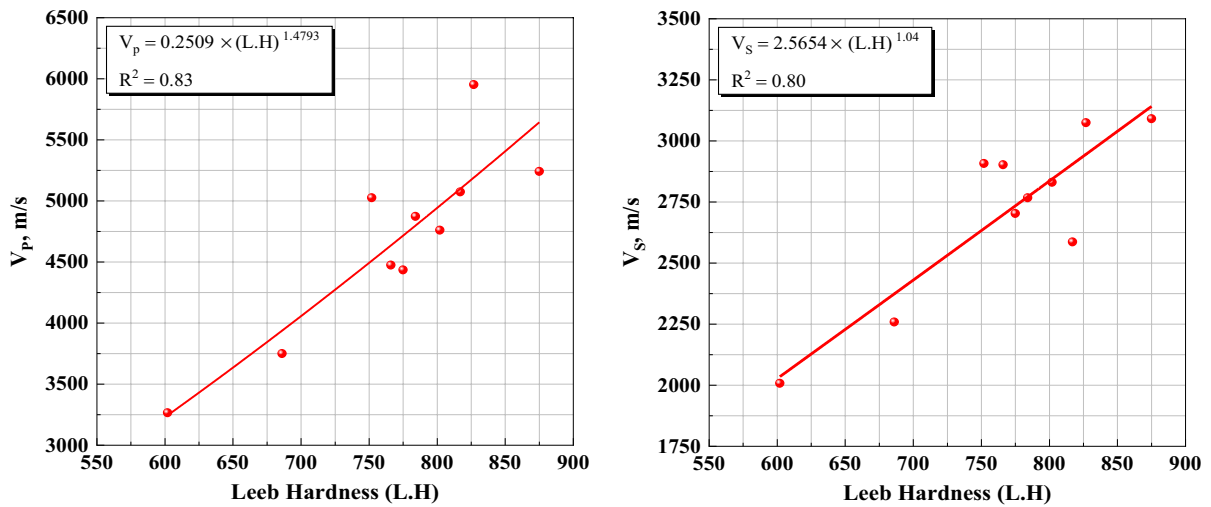
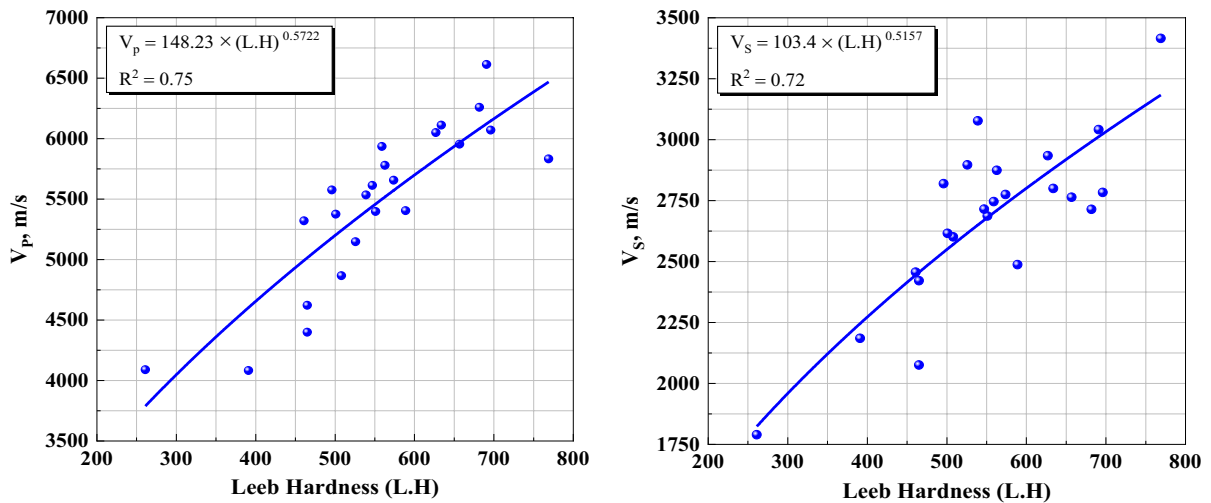


Fig. 2 Distribution curve and frequency histograms of the  $V_p$  and  $V_s$ , dynamic elastic constants, and Leeb hardness



**Fig. 3** Relationship between the  $V_p$  and  $V_s$  with Leeb hardness in igneous rocks



**Fig. 4** Relationship between the  $V_p$  and  $V_s$  with Leeb hardness in sedimentary rocks

regression analysis should be performed separately in both types of samples.

The regression analyses show that all the proposed relationships between dynamic elastic constants and Leeb hardness also follow power functions. The results show that the dynamic modulus of elasticity has the highest coefficients of correlation ( $R^2=0.87$ ) with the Leeb dynamic hardness in igneous rock samples. But, among the dynamic elastic constants in sedimentary rock samples, the bulk modulus ( $K_d$ ) had no very strong correlation

with Leeb hardness. This could mean that the way the variables were distributed did not represent a very significant correlation because the sedimentary samples had high percentages of porosity.

In total, considering different ranges, logic, and mechanisms behind each studied rock hardness testing method, it is found that; various dynamic elastic constants can be determined with the fast, portable, and cheap hardness testing method, Leeb using the relationships presented in Figs. 6, 7 and 8.

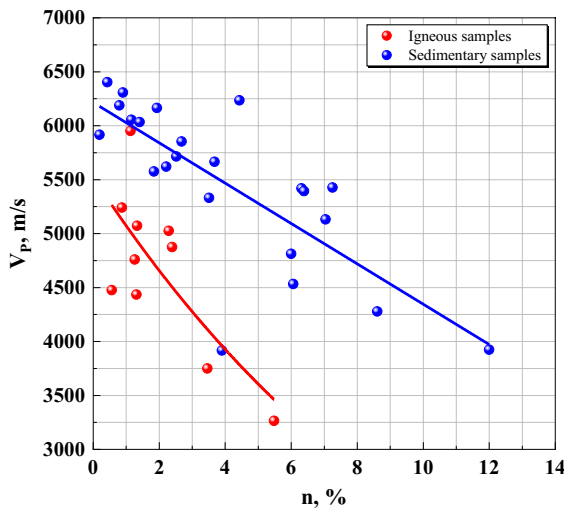


Fig. 5 Dependence of the  $V_p$  data on the porosity

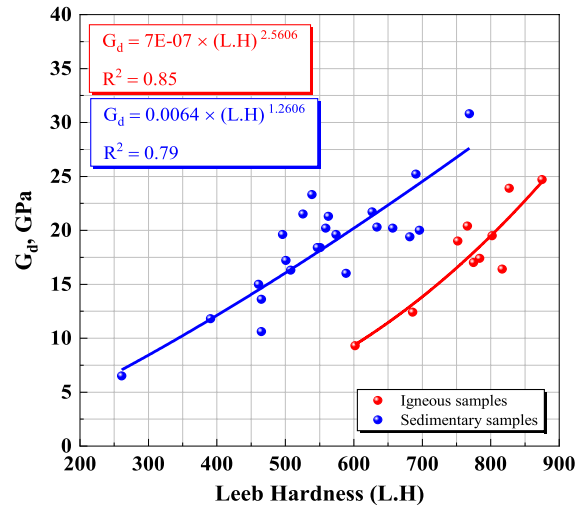


Fig. 7 Relationship between the dynamic modulus of rigidity and Leeb hardness

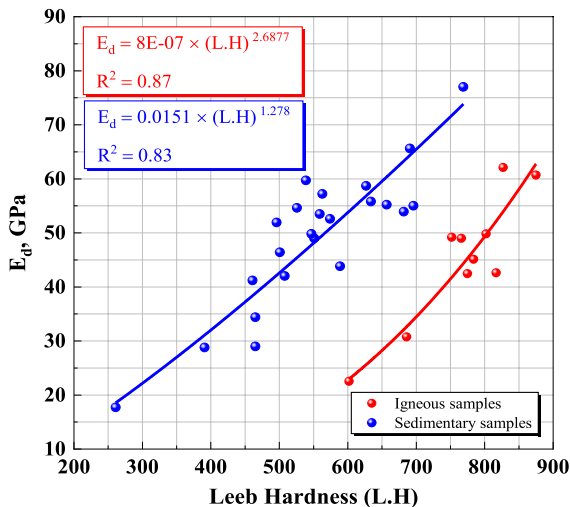


Fig. 6 Relationship between the dynamic modulus of elasticity and Leeb hardness

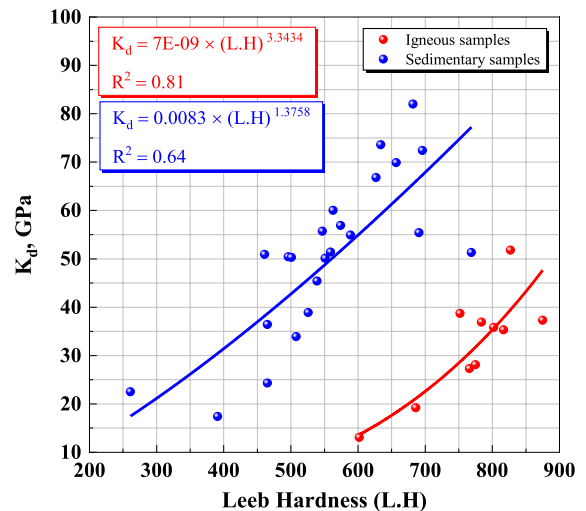


Fig. 8 Relationship between the dynamic bulk modulus and Leeb hardness

### 4.3 The Validity of the Proposed Empirical Equations

The validity of the proposed empirical equations was assessed using common statistical techniques including the correlation coefficient ( $R^2$ ), adjusted R square ( $Adj.R^2$ ), standard error of the estimate (SEE), and analysis of variance (ANOVA). The  $R^2$  and  $Adj.R^2$  are two important indicators that are used to evaluate the validity of regression models

and also the measurement of the strength of the relationship (Kamani and Ajalloeian 2019). The coefficient of determination is the proportion of variation in the dependent variable explained by the regression model. Small values indicate that the model does not fit the data well. On the other side, only the higher value of  $R^2$  is not sufficient for comparison between two regression models because it is not clear whether the higher value of  $R^2$  is due to

the regression model capitalizing or chance with an unknown extra parameter.

On the other hand, F-statistic which is known as F or F-value is suitable for comparison between two regression models. When the F value is large and the significance level is small (typically smaller than 0.05 or 0.01) the null hypothesis could be rejected (Kamani and Ajalloeian 2019). The lower significance level indicates that the results probably are not due to random chance. According to the above-mentioned descriptions, the Adj.  $R^2$ , SEE and ANOVA tests are conducted in this paper to get more efficient correlation and predictive models.

To choose the best predictive model, the regression equation should possess certain statistical parameters. Generally, the best model to be selected should pass the ANOVA tests regarding F-test with a pre-selected significance value (usually Sig. of F is lower than 0.05); have a low value of SEE, and possess a high value of  $R^2$  and Adj.  $R^2$ . Statistical analyses in both igneous and sedimentary rock samples were conducted and the results are presented in Tables 3 and 4.

As shown in Tables 3 and 4, the values of the R,  $R^2$ , and Adj.  $R^2$  between the Leeb dynamic hardness and the dynamic elastic constants in igneous rocks are

greater than in sedimentary rocks. In contrast, the values of SEE in igneous rocks are less than sedimentary rocks. Statistically speaking, a model is considered a better fit when the Sig < 0.05. If Sig > 0.05, a model is not considered to be statistically significant. Therefore, all the relationships presented in Tables 3 and 4 are statistically significant. Additionally, using power models for sedimentary and igneous rock samples gives small errors compared with other models (linear, exponential, and logarithmic). The obtained SEE values of igneous samples range from 0.05 to 0.18 while these errors range from 0.07 to 0.24 for sedimentary samples.

## 5 Microstructure Effects on the Variation of the Leeb Hardness Values

For a better understanding of the influence of microstructure on the Leeb dynamic hardness, the quality index of the rocks has been calculated and investigated. In other words, one of the main questions is what are the dominant parameters affecting the Leeb hardness values? To answer this question, the

**Table 3** Summary of different regression models fitted to five studied parameters with Leeb hardness in igneous samples

Model	Equation	R	$R^2$	Adj. $R^2$	SEE	F	Sig. of F
1	$V_p = 0.2509 \times (L.H)^{1.4793}$	0.91	0.83	0.81	0.07	39.10	0.00
2	$V_s = 2.5654 \times (L.H)^{1.04}$	0.90	0.80	0.78	0.05	32.47	0.00
3	$E_d = 8E - 07 \times (L.H)^{2.6877}$	0.93	0.87	0.85	0.11	52.92	0.00
4	$G_d = 7E - 07 \times (L.H)^{2.5606}$	0.92	0.85	0.83	0.12	44.82	0.00
5	$K_d = 7E - 09 \times (L.H)^{3.3434}$	0.90	0.81	0.78	0.18	32.41	0.00

R, Correlation coefficient;  $R^2$ , Coefficient of determination; Adj.  $R^2$ , adjusted R square; SEE, standard error of the estimate; Sig. of F, Significance of F

**Table 4** Summary of different regression models fitted to five studied parameters with Leeb hardness in sedimentary samples

Model	Equation	R	$R^2$	Adj. $R^2$	SEE	F	Sig. of F
1	$V_p = 148.23 \times (L.H)^{0.5722}$	0.86	0.75	0.74	0.08	62.26	0.00
2	$V_s = 103.4 \times (L.H)^{0.5157}$	0.85	0.72	0.71	0.07	53.94	0.00
3	$E_d = 0.0151 \times (L.H)^{1.278}$	0.91	0.83	0.82	0.13	99.93	0.00
4	$G_d = 0.0064 \times (L.H)^{1.2606}$	0.89	0.79	0.78	0.15	78.52	0.00
5	$K_d = 0.0083 \times (L.H)^{1.3758}$	0.80	0.64	0.62	0.24	36.42	0.00

R, Correlation coefficient;  $R^2$ , Coefficient of determination; Adj.  $R^2$ , adjusted R square; SEE, standard error of the estimate; Sig. of F, Significance of F

microstructure and more detailed examination of the samples has been performed.

The quality index of rocks is calculated directly from laboratory experiments and indirectly using petrographic analysis. So, based on the mineralogical description of rocks, the percentage of minerals for each rock sample was determined. Thereafter, using Eqs. (5) and (6), the longitudinal wave velocity of the rocks ( $V_1^*$ ) and the quality index of the samples were measured. Based on the porosity and the quality index of the sedimentary rocks, the fissuring status of the samples was determined in Fig. 9. As shown in this Figure, all sedimentary

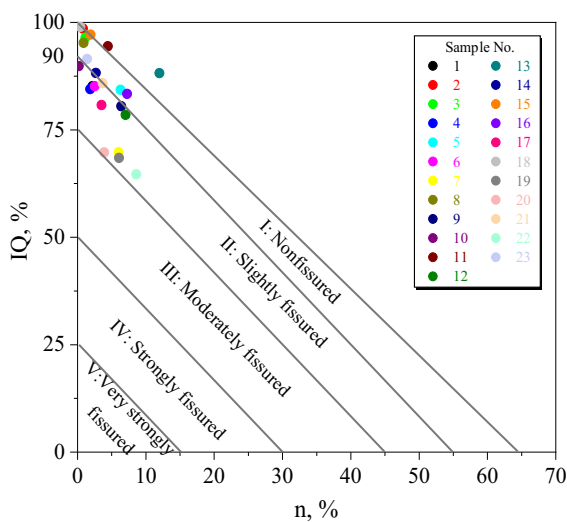


**Fig. 9** Plotting IQ versus porosity for sedimentary samples

samples are in the "slightly" fissured and "non-fissured" categories. Furthermore, two rock samples No.18 (highest quality index and low porosity) and sample No.22 (lowest rock quality index and high porosity) were subjected to microstructure analysis. By examining the thin sections of these two rocks, as shown in Fig. 10, the porosity in the specimen reduces the longitudinal wave velocity, the rock quality index, and finally the Leeb hardness by approximately 32% compared to sample No.18. In other words, in the sample with a low-quality index, the wave is damped in the pores, and the produced rebound velocity is lower, therefore the Leeb hardness reduces. In general, it can be concluded that in sedimentary rocks, the porosity is a dominant factor in the reduction of the Leeb hardness.

Examination of thin sections of igneous samples showed that the intercrystalline and intracrystalline fissures play an important role in changing the Leeb hardness values. These fissures reduce the overall longitudinal velocity of the samples, the rock quality index, and finally reduce the Leeb hardness of the samples. The fissuring status and the related category of 10 igneous samples were determined in Fig. 11. As shown in this Figure, sample No.28 has the lowest quality index and the highest porosity and is in the "moderate quality" category. Therefore, it can be concluded that intercrystalline fissuring has a significant effect on the longitudinal velocity and the quality index of igneous rocks. As a result, the hardness value decreased by 27% in sample No.28 in comparison with sample No.25. Figure 12 shows

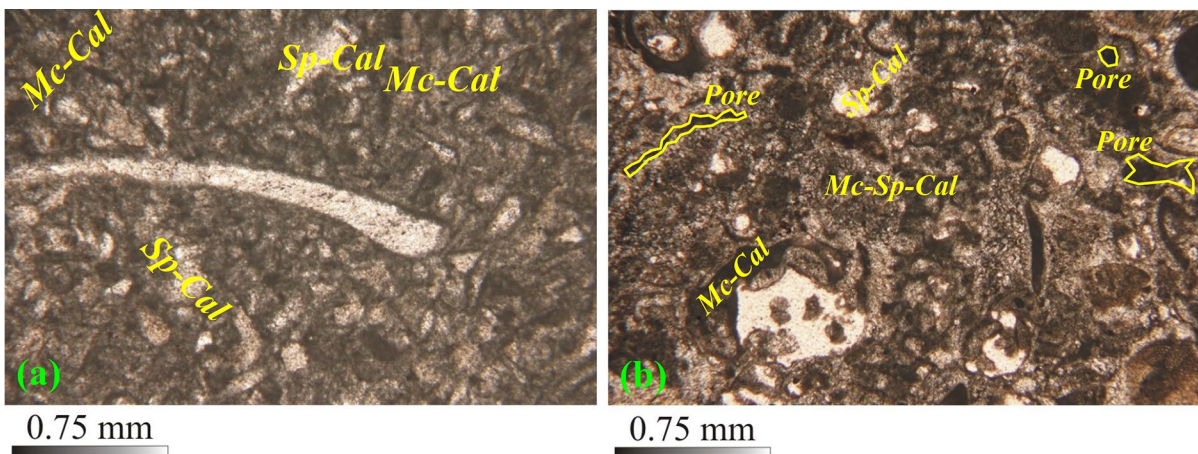


**Fig. 10** Microphotograph of (a) sample No.18 (b) sample No.22



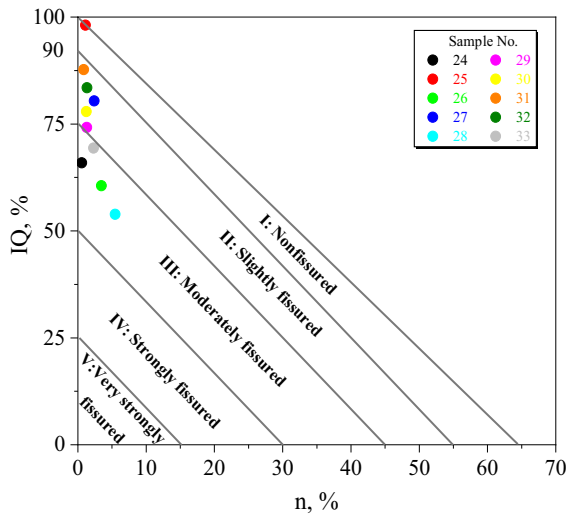


**Fig. 11** Plotting IQ versus porosity for igneous samples

the thin sections of rocks Nos. 28 and 25 considering the intracrystalline and intercrystalline fissures.

According to the above descriptions, it was found that the Leeb dynamic hardness is a function of the

quality index and the quality index is also a function of porosity, so there is a meaningful relationship between these three parameters. In other words, it can be said that  $L.H = f(IQ, n)$ . For this purpose, multiple linear and nonlinear regression analyses between Leeb hardness with porosity and quality index of rocks were performed using the IBM SPSS statistical software version 22.0 (SPSS Inc.). The four functions of linear, logarithmic, power, and exponential have been used to determine the best equations. Tables 5 and 6 show the results of multiple analyses between the three parameters in igneous and sedimentary rocks, respectively. As can be seen, the Leeb hardness parameter is very closely related to the two parameters of porosity and quality index. These relationships are observed in igneous and sedimentary rocks as power. Also, the effect of porosity and rock quality parameters on the Leeb hardness is justified based on high values of  $R^2$ . Therefore, the effect of porosity and quality index of rock samples in measuring the Leeb dynamic hardness is undeniable. Of course, it is necessary to mention that based on the data analyses, it has been shown that the intensity of the effect

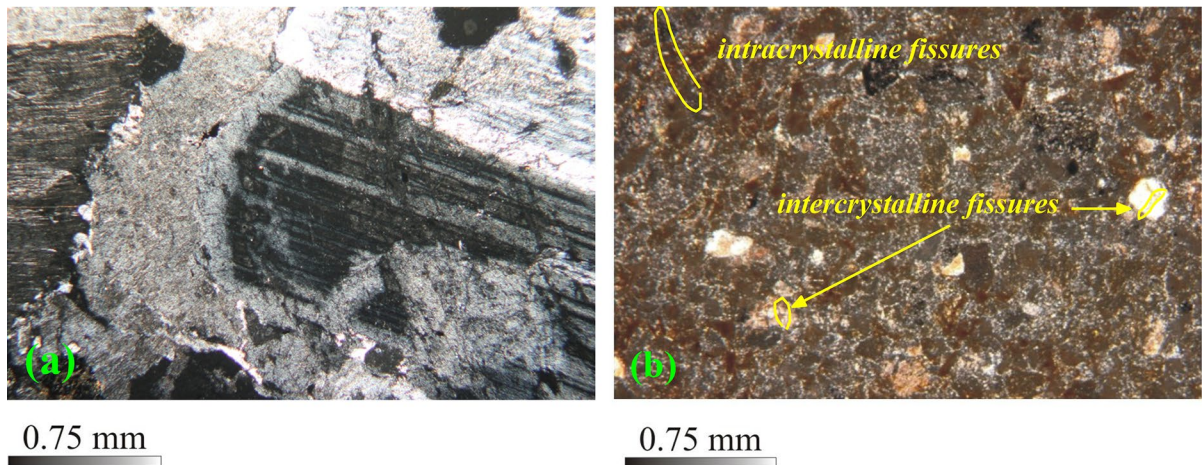


**Fig. 12** Microphotograph of (a) sample No.25 (b) sample No.28

**Table 5** Summary of different multiple regression models between Leeb hardness, porosity, and IQ in igneous samples

Model no	Function	Equation	R <sup>2</sup>
1	Linear	$L.H = 602.794 + 2.959(IQ) - 28.158(n)$	0.94
2	Logarithmic	$L.H = -490.139 + 297.173 \ln(IQ) - 42.638 \ln(n)$	0.93
3	Power	$L.H = 242.672 (IQ)^{0.28} - 16.985 (n)^{1.236}$	0.95
4	Exponential	$L.H = 230.633 e^{0.007IQ} + 437.635 e^{-0.084n}$	0.93

**Table 6** Summary of different multiple regression models between Leeb hardness, porosity, and IQ in sedimentary samples

Model no	Function	Equation	R <sup>2</sup>
1	Linear	$L.H = 354.882 + 3.325(IQ) - 21.076(n)$	0.62
2	Logarithmic	$L.H = -248.126 + 196.513Ln(IQ) - 69.868Ln(n)$	0.64
3	Power	$L.H = 1.995E - 7(IQ)^{4.401} + 545.524(n)^{-0.124}$	0.65
4	Exponential	$L.H = 0.032e^{0.084IQ} + 585.151e^{-0.041n}$	0.62

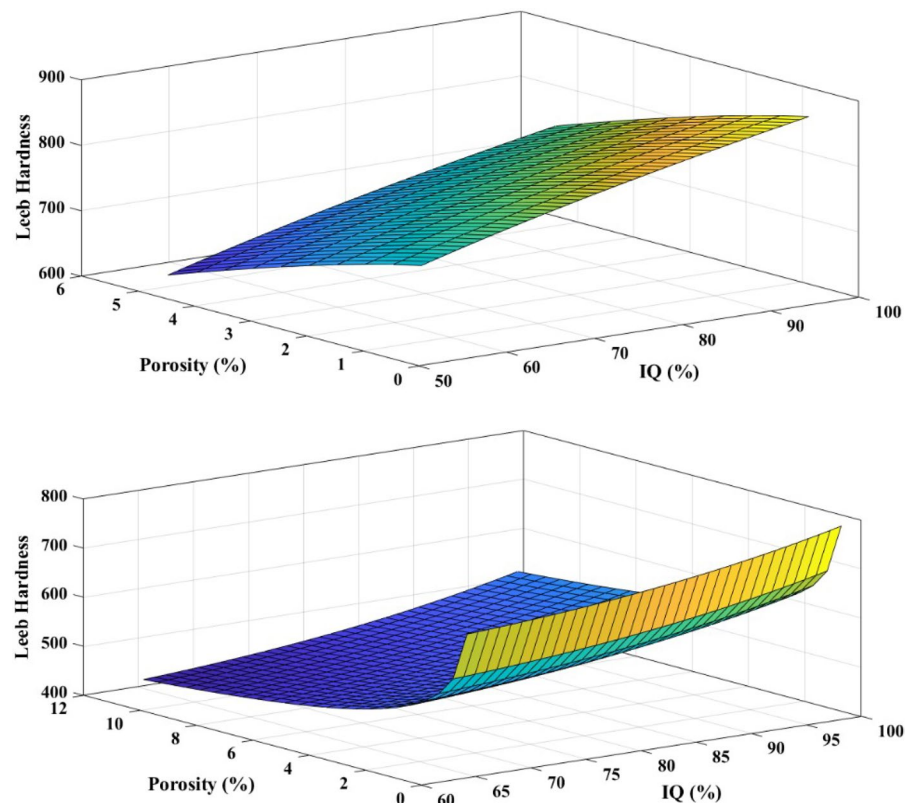
of porosity and rock quality index on the Leeb hardness in igneous samples is more than sedimentary samples.

Figure 13 shows the results of the Leeb hardness tests for the igneous and sedimentary samples with the porosity and IQ values. As can be seen in these Figures, Leeb’s dynamic hardness values increase with increasing the IQ and decreasing the porosity of specimens.

### 6 Longitudinal Waveform in Rock Samples with Different Classes of Leeb Hardness and IQ

Based on the results of statistical analyses in previous sections, it was observed that the  $V_p$  of the sedimentary and igneous rocks has significant relationships with the Leeb dynamic hardness. Therefore, in this section, the longitudinal waveform in the igneous and sedimentary rocks have been investigated considering their Leeb hardness and IQ values. For this purpose, the longitudinal waveforms of four samples No. 2, No. 18, No. 19, and No. 22 in sedimentary rocks and samples No. 25, No. 26, No. 28, and No. 31 in igneous rocks were analyzed.

**Fig. 13** The average Leeb hardness of rock specimens correlated with the porosity with various IQ values (top) igneous samples (bottom) sedimentary samples



Based on the shape of longitudinal waves in samples No. 2, No. 18, No. 19, and No. 22 as shown in Fig. 14, it could be concluded that in samples with a high-quality index and high Leeb dynamic hardness value, the wave amplitude is large. One of the reasons for the low longitudinal wave amplitude in samples No. 19 and No. 22 compared to samples No. 2 and No. 18 is its high porosity. In other words, the existence of high porosity in samples No. 22 and No. 19 compared to samples No. 18 and No. 2 damps the wave penetration into the sample's internal structure, which leads to a decrease in the Leeb

hardness and the longitudinal wave in it. Therefore, in general, the existence of porosity reduces the wave amplitude in samples with low Leeb hardness.

The same results were observed in igneous samples (see Fig. 15). In samples No. 25 and No. 31 which have higher IQ and Leeb hardness values, higher values of wave amplitude have been observed compared with samples No. 28 and No. 26. Generally, the role of porosity in sedimentary rocks and fissuring in igneous rocks are effective in variation the Leeb dynamic hardness and consequently, the form of the received longitudinal waves.

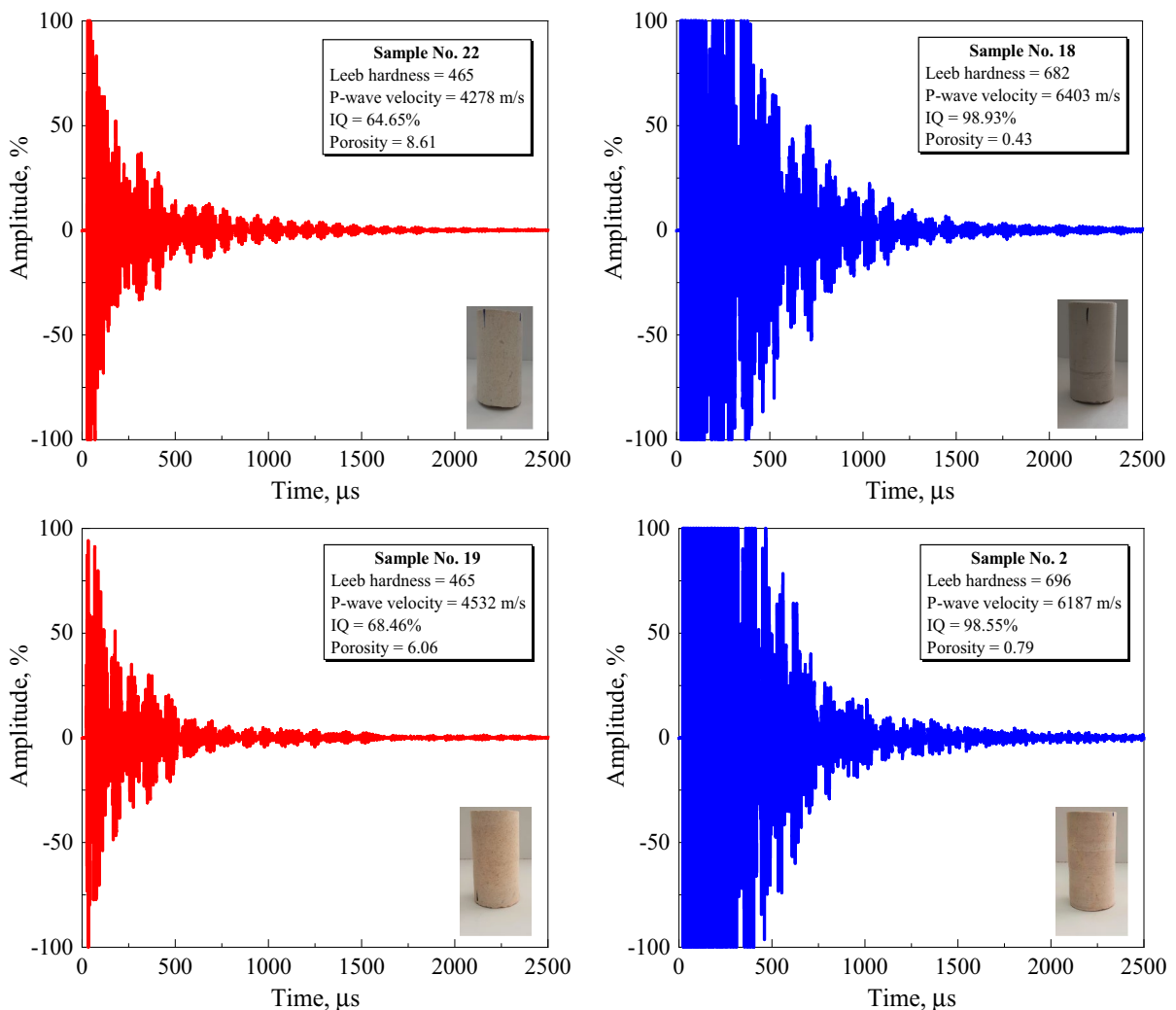


**Fig. 14** A comparison of P-wave forms between sedimentary specimens with different Leeb hardness and IQ

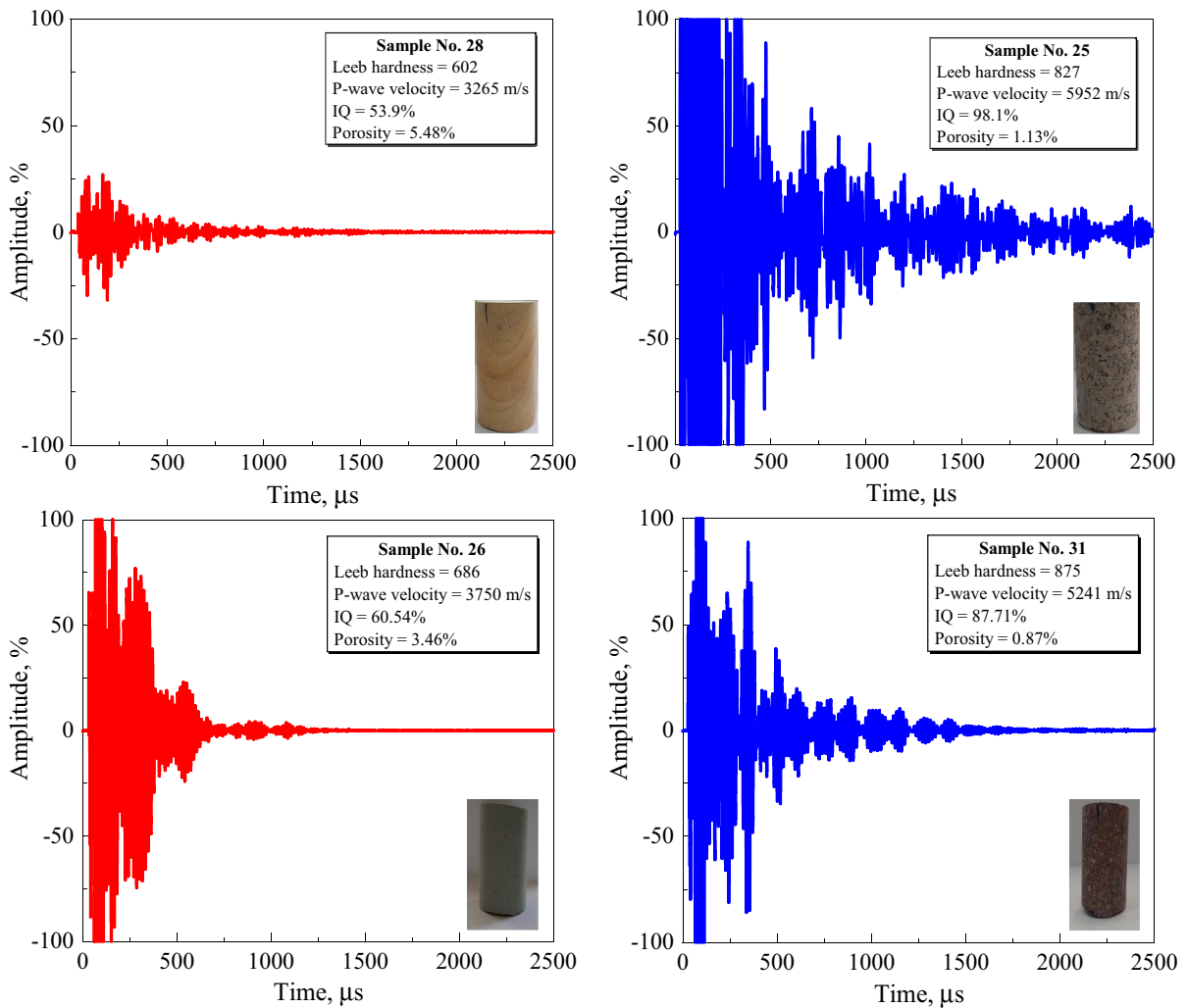


**Fig. 15** A comparison of P-wave forms between igneous specimens with different Leeb hardness and IQ

## 7 Conclusions

This study has presented, for the first time, a study of the application of the portable Leeb hardness testing technique in the prediction of the dynamic elastic constants of igneous and sedimentary rocks. Variation in Leeb hardness and longitudinal waveforms of igneous and sedimentary rocks were also analyzed based on the quality index (IQ). Some of the important outputs of this paper are as follows:

- The results of statistical analyses show that in both igneous and sedimentary rocks, the Leeb hardness has a significant correlation with the dynamic

modulus of elasticity ( $E_d$ ) with the correlation coefficients of 0.87 and 0.83, respectively.

- Based on the analysis of IQ-porosity plots, it was observed that porosity in sedimentary rocks and fissuring in igneous rocks have a great effect on the variation of the Leeb dynamic hardness. In other words, sedimentary rocks with a low-quality index and high porosity cause the lower Leeb hardness. Also in igneous rocks, intercrystalline and intracrystalline fissures reduce the quality index of the rock and consequently result in a reduction in the Leeb dynamic hardness.
- By examining the longitudinal waveforms in igneous and sedimentary rocks, it was observed that

the amplitude of the longitudinal waves is shorter in samples with low Leeb hardness and quality index.

**Funding** The authors have not disclosed any funding.

**Data Availability** Enquiries about data availability should be directed to the authors.

#### Declarations

**Conflict of interests** The authors declare that they have no known competing financial interests or personal relationships that could have appeared to influence the work reported in this paper.

#### References

- Ajalloeian R, Jamshidi A, Khorasani R (2020) Assessments of ultrasonic pulse velocity and dynamic elastic constants of granitic rocks using petrographic characteristics. *Geotech Geol Eng* 38:2835–2844. <https://doi.org/10.1007/s10706-020-01189-6>
- Aldeeky H, Al Hattamleh O, Rababah S (2020) Assessing the uniaxial compressive strength and tangent Young's modulus of basalt rock using the Leeb rebound hardness test. *Mater Constr* 70:230. <https://doi.org/10.3989/mc.2020.15119>
- Aoki H, Matsukura Y (2007) A new technique for non-destructive field measurement of rock-surface strength: an application of the Equotip hardness tester to weathering studies. *Earth Surface Process Landforms J Br Geomorph Res Group* 32:1759–1769. <https://doi.org/10.1002/esp.1492>
- Aoki H, Matsukura Y (2008) Estimating the unconfined compressive strength of intact rocks from Equotip hardness. *Bull Eng Geol Env* 67:23–29. <https://doi.org/10.1007/s10064-007-0116-z>
- ASTM A956-06 (2006) Standard test method for leeb hardness testing of steel products. West Conshohocken, PA
- Azimian A (2017) Application of statistical methods for predicting uniaxial compressive strength of limestone rocks using nondestructive tests. *Acta Geotech* 12:321–333. <https://doi.org/10.1007/s11440-016-0467-3>
- Bandini A, Berry P (2013) Influence of marble's texture on its mechanical behavior. *Rock Mech Rock Eng* 46:785–799. <https://doi.org/10.1007/s00603-012-0315-1>
- Benavente D, Fort R, Gomez-Heras M (2021) Improving uniaxial compressive strength estimation of carbonate sedimentary rocks by combining minimally invasive and non-destructive techniques. *Int J Rock Mech Min Sci* 147:104915. <https://doi.org/10.1016/j.ijrmms.2021.104915>
- Çelik SB, Çobanoğlu İ (2019) Comparative investigation of Shore, Schmidt, and Leeb hardness tests in the characterization of rock materials. *Environ Earth Sci* 78:554. <https://doi.org/10.1007/s12665-019-8567-7>
- Çelik SB, Çobanoğlu İ, Koralay T (2020) Investigation of the use of Leeb hardness in the estimation of some physical and mechanical properties of rock materials. *Pamukkale Üniversitesi Mühendislik Bilimleri Dergisi* 26:1385–1392. <https://doi.org/10.5505/pajes.2020.22747>
- Corkum AG, Asiri Y, El Naggar H, Kinakin D (2018) The Leeb hardness test for rock: an updated methodology and UCS correlation. *Rock Mech Rock Eng* 51:665–675. <https://doi.org/10.1007/s00603-017-1372-2>
- Davarpanah SM, Ván P, Vásárhelyi B (2020) Investigation of the relationship between dynamic and static deformation moduli of rocks. *Geomech Geophys Geo-Energy Geo-Resour* 6:1–14. <https://doi.org/10.1007/s40948-020-00155-z>
- Dehghani B, Amirkiyaei V, Ebrahimi R et al (2020) Thermal loading effect on P-wave form and power spectral density in crystalline and non-crystalline rocks. *Arab J Geosci* 13:1–9. <https://doi.org/10.1007/s12517-020-05779-9>
- Desarnaud J, Kiriyaama K, Bicer Simsir B et al (2019) A laboratory study of Equotip surface hardness measurements on a range of sandstones: What influences the values and what do they mean? *Earth Surf Proc Land* 44:1419–1429. <https://doi.org/10.1002/esp.4584>
- Diamantis K, Gartzos E, Migiros G (2009) Study on uniaxial compressive strength, point load strength index, dynamic and physical properties of serpentinites from Central Greece: test results and empirical relations. *Eng Geol* 108:199–207. <https://doi.org/10.1007/s11440-016-0467-3>
- Fereidooni D (2018) Assessing the effects of mineral content and porosity on ultrasonic wave velocity. *Geomech Eng* 14:399–406. <https://doi.org/10.12989/gae.2018.14.4.399>
- Fourmaintraux D (1976) Characterization of rocks: laboratory tests. *La Mécanique des roches applique aux ouvrages du génie civil*. Ecole Nationale des Pontset Chaussées, Paris
- Frank S, Frehner C, Akhlaghi A (2019) Portable hardness testing: Leeb, portable rockwell and UCI, Equotip Application Booklet, Proceq SA
- Garrido ME, Petnga FB, Martínez-Ibáñez V et al (2021) Predicting the uniaxial compressive strength of a limestone exposed to high temperatures by point load and Leeb rebound hardness testing. *Rock Mech Rock Eng*. <https://doi.org/10.1007/s00603-021-02647-0>
- Gokceoglu C, Zorlu K (2004) A fuzzy model to predict the uniaxial compressive strength and the modulus of elasticity of a problematic rock. *Eng Appl Artif Intell* 17:61–72. <https://doi.org/10.1016/j.engappai.2003.11.006>
- Gomez-Heras M, Benavente D, Pla C et al (2020) Ultrasonic pulse velocity as a way of improving uniaxial compressive strength estimations from Leeb hardness measurements. *Constr Build Mater* 261:119996. <https://doi.org/10.1016/j.conbuildmat.2020.119996>
- Goodman RE (1989) Introduction to rock mechanics, 2nd edn. Wiley, New York
- Gupta V (2009) Non-destructive testing of some Higher Himalayan Rocks in the Satluj Valley. *Bull Eng Geol Env* 68:409–416. <https://doi.org/10.1007/s10064-009-0211-4>
- Hack H, Hingira J, Verwaal W (1993) Determination of discontinuity wall strength by Equotip and ball rebound tests. *Int J Rock Mech Min Sci Geomech Abstracts* 30:151. [https://doi.org/10.1016/0148-9062\(93\)90707-K](https://doi.org/10.1016/0148-9062(93)90707-K)

- İnce İ, Bozdağ A (2021) An investigation on sample size in Leeb hardness test and prediction of some index properties of magmatic rocks. *Arab J Geosci* 14:1–13. <https://doi.org/10.1007/s12517-021-06478-9>
- ISRM (1981) *Rock characterisation, testing and monitoring*. Pergamon Press, Oxford
- ISRM (2015) *The ISRM suggested methods for rock characterization, testing and monitoring: 2007–2014*. Ankara, Turkey
- Jamshidi A, Torabi-Kaveh M (2021) Anisotropy in ultrasonic pulse velocity and dynamic elastic constants of laminated sandstone. *Q J Eng GeolHydrogeol* 54:1–9. <https://doi.org/10.1144/qjegh2020-101>
- Jamshidi A, Yazarloo R (2021) Influence of rock specimen diameter size on the ultrasonic pulse velocity and dynamic elastic constants. *Geopersia* 11:361–376. <https://doi.org/10.22059/GEOPE.2021.317191.648592>
- Kamani M, Ajalloeian R (2019) Evaluation of engineering properties of some carbonate rocks through corrected texture coefficient. *Geotech Geol Eng* 37:599–614. <https://doi.org/10.1007/s10706-018-0630-8>
- Karaman K, Kesimal A (2015) Correlation of Schmidt rebound hardness with uniaxial compressive strength and P-wave velocity of rock materials. *Arab J Sci Eng* 40:1897–1906. <https://doi.org/10.1007/s13369-014-1510-z>
- Kelsall PC, Watters RJ, Franzone JG (1986) Engineering characterization of fissured, weathered dolerite and vesicular basalt. In: *The 27th US Symposium on Rock Mechanics (USRMS)*
- Khandelwal M (2013) Correlating P-wave velocity with the physico-mechanical properties of different rocks. *Pure Appl Geophys* 170:507–514. <https://doi.org/10.1007/s00024-012-0556-7>
- Leeb D (1978) New dynamic method for hardness testing of metallic materials. *Rev Metal* 15:123–128
- Martínez-Martínez J, Benavente D, García-del-Cura MA (2012) Comparison of the static and dynamic elastic modulus in carbonate rocks. *Bull Eng Geol Env* 71:263–268. <https://doi.org/10.1007/s10064-011-0399-y>
- Meulenkamp F, Grima MA (1999) Application of neural networks for the prediction of the unconfined compressive strength (UCS) from Equotip hardness. *Int J Rock Mech Min Sci* 36:29–39. [https://doi.org/10.1016/S0148-9062\(98\)00173-9](https://doi.org/10.1016/S0148-9062(98)00173-9)
- Sharma PK, Khandelwal M, Singh TN (2011) A correlation between Schmidt hammer rebound numbers with impact strength index, slake durability index and P-wave velocity. *Int J Earth Sci* 100:189–195. <https://doi.org/10.1007/s00531-009-0506-5>
- Sousa LMO (2014) Petrophysical properties and durability of granites employed as building stone: a comprehensive evaluation. *Bull Eng Geol Env* 73:569–588. <https://doi.org/10.1007/s10064-013-0553-9>
- Viles H, Goudie A, Grab S, Lalley J (2011) The use of the Schmidt Hammer and Equotip for rock hardness assessment in geomorphology and heritage science: a comparative analysis. *Earth Surf Proc Land* 36:320–333. <https://doi.org/10.1002/esp.2040>
- Yagiz S (2009) Predicting uniaxial compressive strength, modulus of elasticity and index properties of rocks using the Schmidt hammer. *Bull Eng Geol Env* 68:55–63. <https://doi.org/10.1007/s10064-008-0172-z>
- Yilmaz NG (2013) The influence of testing procedures on uniaxial compressive strength prediction of carbonate rocks from Equotip hardness tester (EHT) and proposal of a new testing methodology: hybrid dynamic hardness (HDH). *Rock Mech Rock Eng* 46:95–106. <https://doi.org/10.1007/s00603-012-0261-y>
- Yilmaz NG, Goktan RM (2018) Analysis of the Leeb hardness test data obtained by using two different rock core holders. *J Nat Appl Sci* 22:1–8. <https://doi.org/10.19113/sdufbed.28343>
- Yüksek S (2019) Mechanical properties of some building stones from volcanic deposits of mount Erciyes (Turkey). *Mater Constr* 69:187. <https://doi.org/10.3989/mc.2019.04618>

**Publisher's Note** Springer Nature remains neutral with regard to jurisdictional claims in published maps and institutional affiliations.